

The Magnetoimpedance Effect and Principles of Measuring

Radoslav Surla ^{1*}, Nebojša Mitrović ¹, Jelena Orelj ¹, Vasilija Joksimović ²

¹ University of Kragujevac, Faculty of Technical Sciences Čačak, Serbia

² Military Technical Institute, Belgrade, Serbia

* nebojsa.mitrovic@ftn.kg.ac.rs

Abstract: This paper presents magnetoimpedance (MI) effects and the principles of measuring in order to exhibit the MI dependence on frequency and external magnetic field intensity. This phenomenon is not enough represented in Educational programs so this paper will be used as a learning material of basic concepts, influencing factors and the principles of measuring of MI effect. The obtained MI diagrams are shown for amorphous/nanocrystalline FINEMET type ferromagnetic $\text{Fe}_{72}\text{Cu}_1\text{V}_4\text{Si}_{15}\text{B}_8$ ribbons and $\text{Fe}_{73}\text{Cu}_1\text{Nb}_3\text{Si}_{13.5}\text{B}_{9.5}$ microwires.

Keywords: MI effect, skin effect, amorphous/nanocrystalline ferromagnetic ribbons and microwires

1. INTRODUCTION

Changing magnetic impedance under the influence of an external DC magnetic field is named magnetoimpedance (MI) effect. If the MI ratio is higher than 100 % than it is named the giant magnetoimpedance (GMI) effect. MI effect was discovered in the early nineties of the twentieth century [1] and today is used for making a very sensitive magnetic field sensor whose sensitivity reaches up to about 7% /kA/m [1-7]. Different impedance measurements methods are implemented through the educational system as well as the phenomenon and explanations of the skin effect on the conductor through which flows the alternating current. This paper describes principles in measuring MI effects unifying classical impedance measuring principles which changes under the influence of frequency and external magnetic field. The influence of frequency at the impedance is studied by the skin effect and the influence of the external magnetic field by the domain structure of the material.

1.1. The domain structure of the material under the MI effect

In order to explain the MI effect, it is necessary to analyze the domain structure of the elements in which the effect is studied (e.g., ribbons, wires, films).

For samples in the form of striped parallelepiped, the magnetic domains are arranged along of axis, i.e. at an angle of 90° in relation to the length of the ribbons, as it shown in Fig. 1. Adjacent domains have the opposite orientation, which is caused by achieving the best energy configuration.

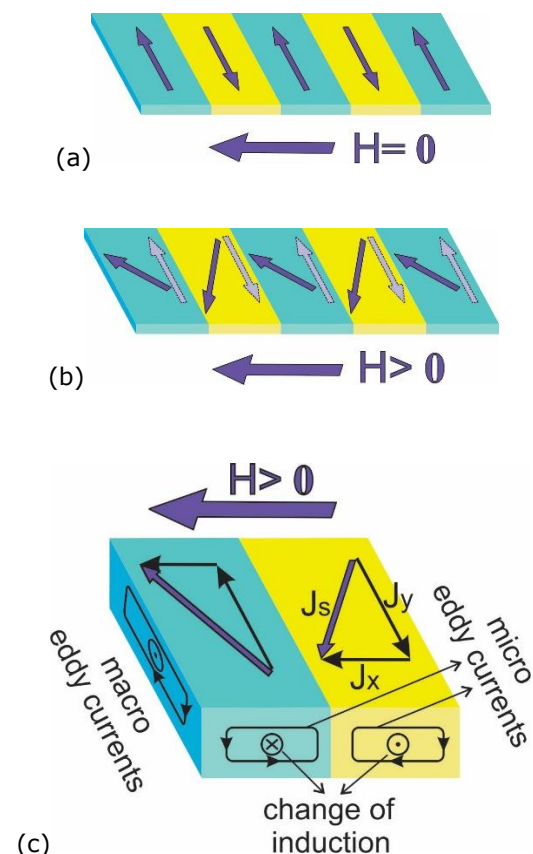


Figure 1. The magnetic domains in amorphous ribbon.

The orientation of magnetic domains in amorphous melt-spun microwires depends on magnetostriction, where it can be positive (for iron-based alloys) or negative (for cobalt based alloys) as it shown in Fig. 2.

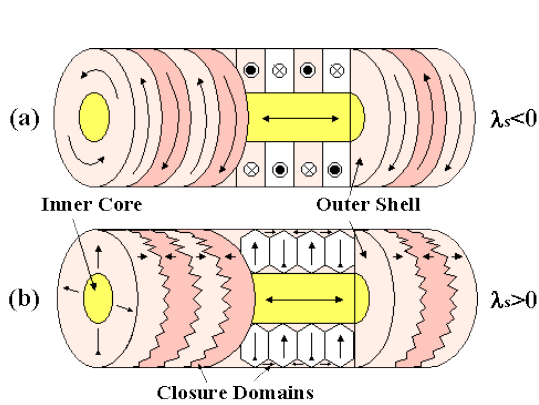


Figure 2. The magnetic domains in amorphous melt-spun wires.

There are also amorphous metal-like glass-covered magnetic wires with a specific magnetic domain arrangement Fig. 3 [8].

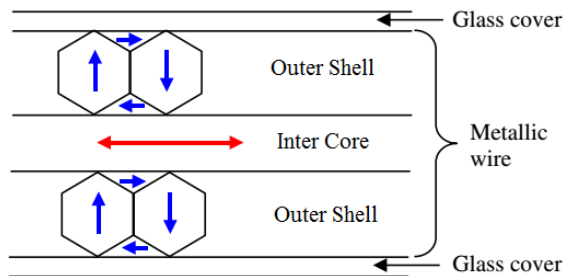


Figure 3. The magnetic domains in amorphous glass-covered magnetic microwires.

1.2. Calculating the MI ratio

Exposing the ferromagnetic material to external dc magnetic field leads to the rotation of the magnetic domains in the direction of the magnetic field what leads to a decrease in the impedance of the sample. Relative change in impedance (Z) of the sample with the change of dc magnetic field (H) is called magnetic-impedance (MI) ratio and is defined as:

$$\frac{\Delta Z}{Z} = 100\% \cdot \frac{Z(H) - Z(H_{max})}{Z(H_{max})}, \quad (1)$$

where $Z(H)$ is impedance at a certain value of the magnetic field, and $Z(H_{max})$ is the impedance at the maximum magnetic field that depends on measuring equipment.

1.2. Influence of frequency on MI effect

Changing the frequency leads to the change of the impedance according to skin effect (see Fig. 4), given by the following equation [9]:

$$\delta_m = \sqrt{\frac{\rho}{\pi \cdot \mu \cdot f}}, \quad (2)$$

where are

- δ_m – penetration depth (skin effect)
- ρ – electrical resistivity,
- μ – magnetic permeability, and
- f – frequency.

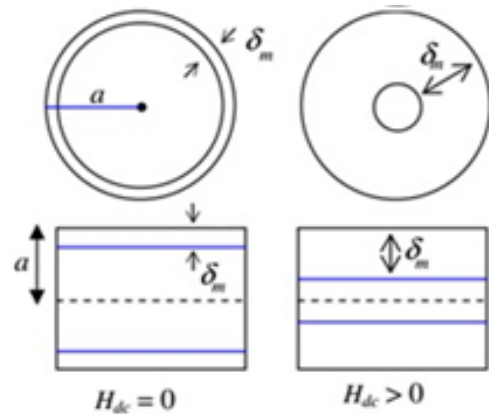
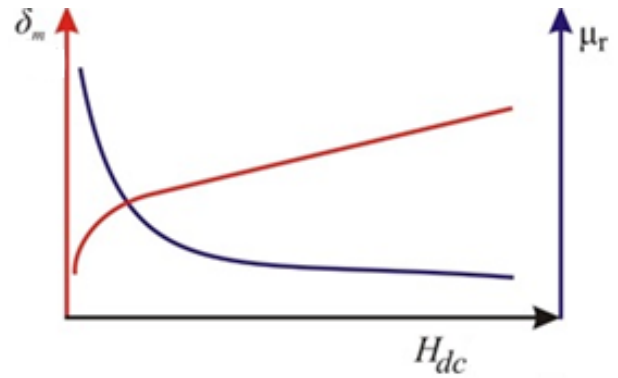


Figure 4. Penetration depth changes in microwires depending on external dc magnetic field [10].

In the soft magnetic material with high permeability values and lower values of the electrical resistivity, at a relatively high frequency, penetration depth becomes less than half the thickness of the ribbon, i.e. the radius of the microwire. The cutoff frequency at which this is happening and MI-effect begins is named the critical frequency.

Regarding this, it is important to note that at a certain value of the frequency and magnetic field strength, the maximum value of the MI ratio is reached, so that experimental measurements establish these values that are further used for designing the MI-based sensors.

2. MI measuring principles

Two common instruments used to perform MI measurements are the RLC meter and the Vector Network Analyzer - VNA.

Depending on the principle of impedance measurement there can be defined two methods: using the RLC meter (usually for lower frequencies, up to few MHz) and using the microwave technique by VNA (at higher frequencies up to few GHz).

In the first case the impedance is measured at four points method and it is based on the measurement of the voltage drop at the ends of the sample with the current passing through the same. In the second case it is used the microwave

technique of high-frequency passage of the current through the sample.

2.1. Measuring principle of MI effect by measuring voltage and current

This principle is based on measuring impedance by the four-point method by LCR HiTester, where the voltage and the current are measured on the same sample.

The instrument automatically calculates and displays the results of the impedance. Depending on the type of the instrument, it is possible to get the real and imaginary part of the impedance as well as the results for the different values of the current intensity used in the measurement.

The impedance can be expressed in the complex form by the equation $Z(\omega) = R + jX$, where R and X are a real and complex component of impedance. Its value is obtained by the ratio V_{ac}/I_{ac} . The value of I_{ac} is the amplitude of the current of the sinusoidal form $i = I_{ac} \sin(\omega t)$, and V_{ac} is the voltage amplitude measured at the ends of the sample through which the current flows as it is shown on Fig. 5 [2, 4].

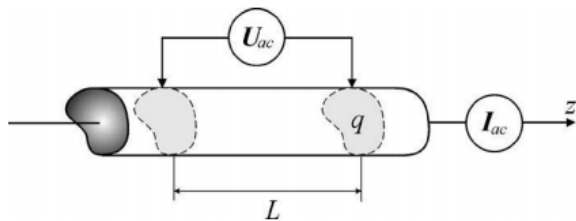


Figure 5. Schematic illustration of impedance measuring using RLC meter.

This impedance definition applies only to the linear segment of ferromagnetic materials and is limited in application. Since the ferromagnetic materials are non-linear, the linear approximation is used to calculate the GMI ratio of ferromagnetic materials of length L and cross-section q [7]:

$$Z = \frac{V_{ac}}{I_{ac}} = \frac{LE_z(S)}{q\langle j_z \rangle_q} = R_{dc} \frac{j_z(S)}{\langle j_z \rangle_q}, \quad (3)$$

where E_z and $j_z(S)$ are longitudinal component of the electrical field and current density, respectively, R_{dc} is a dc resistance of the sample, and $\langle j_z \rangle_q$ is the mean value of the current component through the cross-section q .

The MI ratio can be calculated, for a cylindrical conductor (amorphous or nanocrystalline microwires) by the equation [7]:

$$\frac{Z}{R_{DC}} = ka \frac{J_0(ka)}{2J_1(ka)} \quad (4)$$

where J_0 and J_1 are the Bessel function of the first kind, and for samples in the form of a thin film, or strip [2]:

$$\frac{Z}{R_{DC}} = k \frac{t}{2} \cot(k \frac{t}{2}), \quad (5)$$

where a is the diameter of the wire, t is the thickness of the strip or film. The propagation constant k is defined as $k=(1-i)/\delta_m$, where δ_m is the penetration depth in the classical skin effect defined by the equation (2).

2.2. The principle of MI effect measurements in the microwave technique

It is convenient to realize impedance measuring at higher frequencies using Vector Network Analyzer by the principle of microwave technique [11].

In order to clarify the principle of measurements using the VNA instrument, it is necessary to define the scattering parameters, known as S -parameters which can describe and design the electrical components in microwave devices, as well as adjust the consumers connected to microwave lines. Fig. 6 shows the S -parameters defined in wave propagation between the two ports of the VNA instrument.

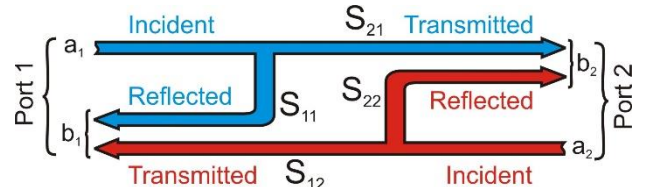


Figure 6 Schematic illustration of the scattering parameters.

According to Fig. 6, S -parameters are defined with two basic relations

$$b_1 = S_{11} \cdot a_1 + S_{12} \cdot a_2 \quad (6)$$

$$b_2 = S_{21} \cdot a_1 + S_{22} \cdot a_2, \quad (7)$$

where S_{11} and S_{22} represent the parameters of reflection and S_{21} and S_{12} represent the parameters of transmission of the signal:

S_{11} - Forward Reflection (input match - impedance)

S_{22} - Reverse Reflection (output match - impedance)

S_{21} - Forward Transmission (gain or loss)

S_{12} - Reverse Transmission (leakage or isolation).

The impedance measurement is performed by connecting a sample ("DUT" - "device under test") with unknown impedance (Z_x) to one or two instrument ports. The results are available on the display using the calculation of the S parameter, depending on sample connection.

The unknown impedance refers to the required calibration of the instrument before measurement, with a special calibration kit that is part of the instrument set. In order to connect the sample to the instrument, it is necessary to design a special

sample holder which dimensions must be in accordance with the frequency range used in the measurement. It is necessary to harmonize the wavelength of the electromagnetic wave λ and the length of the medium through which it extends. Wavelength is calculated according to the form $\lambda=c/f$, ($c=3 \cdot 10^8$ m/s).

Transmission lines play an important role at medium and higher frequencies, and the measured current and voltage are not equal at every point in a line (wires); this cause the appearance of the envelope wave on the measured sample. Therefore, it is more important to pay attention to the characteristic impedance Z_0 of the cables on the VNA instrument.

The characteristic impedance is defined as the ratio of voltage and current at any point of the infinitely long homogeneous conductor, and this value is constant. It can be defined as impedance at the end of the conductor so that the input impedance of conductor is equal to itself. The characteristic impedance is the secondary conductor parameter and is also defined as the geometric mean of the impedance at closed (Z_{sc}) - short connection and open (Z_{∞}) - open connection: $Z_0 = (Z_{sc} \cdot Z_{\infty})^{1/2}$, where it is used $Z_{sc} = R + j\omega L$; $Z_{\infty} = 1/(G + j\omega C)$, so: $Z_0 = [(R + j\omega L)/(G + j\omega C)]^{1/2}$.

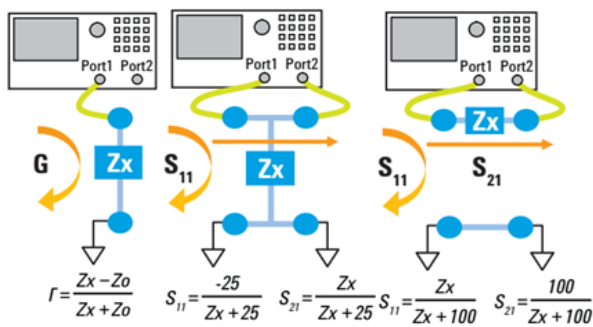


Figure 7. Impedance measurement with VNA instrument with: one port and two ports to different DUT configurations.

In order to realize measurement with VNA, the manufacturer (HP Agilent) defined the use of coaxial cables with $Z_0 = 50 \Omega$, as well as principles for measuring unknown impedance (Z_x), of depending on one, or two or more approaches were used, and depending on principles different S-parameters were used. It is necessary, during the experiment, to make a sample holder that enables the sample connection to one or two ports (see Fig. 7).

The recommended principles are used depending on the value of the unknown impedance. The measurement principle with one instrument port is used for an unknown impedance with close value of Z_0 , where the unknown impedance is determined using the ratio between the unknown and the characteristic impedance.

The principle of shaft (serial connection) is used in the case when the difference between the unknown and characteristic impedance cause the increase of measurement noise. The sample is connected in two ways, by shorting the access (and the middle part of the cable and armor) between which the unknown impedance is connected, as well as by shortening the middle part of the cable through an unknown impedance, and armor directly, without an unknown impedance (see Fig. 7).

One of the designed holder in the shape of microstrip transfer media is realized in such a way that the measured sample with the contacts builds the transmission line, and the under part of the plate is a jumper (entire surface made of copper). There are "SMA 7" connectors at the ends of the sample holder that allow the coaxial cables of the characteristic impedance $Z_0 = 50 \Omega$ to be connected to the VNA instrument (see Fig. 8).

Connection terminals, BNC and NC connectors are also used in practice in order to provide correct connections to the connection cables, but the selection of connectors depends on the frequency of the signal used during the measurement.

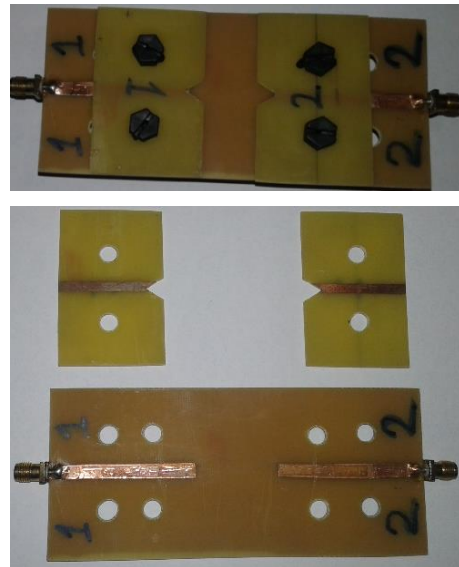


Figure 8. Sample holder in the form of microstrip transfer media for measuring the MI effect.

3. MI EFFECT DIAGRAM APPERANCE

Depending on the measurement equipment and the acquisition of the results, it is possible to obtain MI diagrams that are described with a lot of points, which enables a more precise and quality monitoring of the results. For example, VNA instrument can measure 1601 different values of the impedance in a single sweep, depending on the frequency range (with a linear or logarithmic distribution).

The results are visible on the instrument display (see Fig. 9), but the instrument also record the

results in a separate file format on the external memory. The instrument has the option to save the first measurement as a state and to display it as a baseline diagram on the monitor at the same time as currently measured values. This enables control of the correctness of the measurement and orientation monitoring of the MI effect during the measuring.

During the experiment, after recording a single measurement cycle that impedance is reduced when the sample is exposed to a magnetic field that gradually increases to a maximum value.



Figure 9. Display of the results of impedance measurement using VNA.

The first measurement cycle is completed after reaching the maximum field value (in the case of $H_{max} = +21.8$ kA/m). When the next measurement cycle starts the sample is not subjected to field effect ($H = 0$). The value of the impedance in this case is lower than in the initial measurement when the field is also $H = 0$. The cause is retained magnetization that has remained after previously occurred magnetization of the sample.

When the sample is exposed to the opposite field that gradually increases, for example to $H_{max} = -21.8$ kA/m and the impedance is remeasured at $H = 0$ (after the second measurement cycle), almost identical results of the measured impedance are obtained, as in the first cycle, where: $0 < \Delta Z < 0.03 \Omega$ (see Fig. 10).

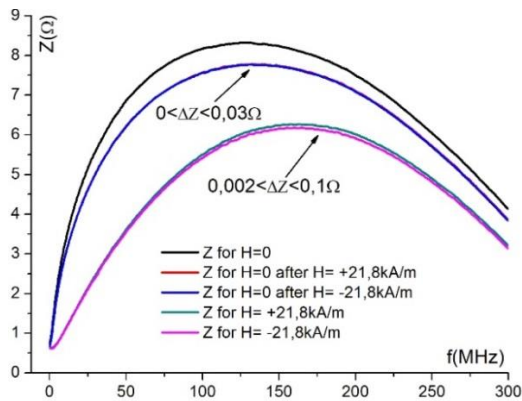


Figure 10. Impedance of $Fe_{72}Cu_1V_4Si_{15}B_8$ ribbons annealed at $500^\circ C$ of depending on the $H=0$, or $H_{max} = \pm 21.8$ kA/m before and after two measurement cycles.

Approximately the same impedance values are obtained at identical values of the magnetic field, but in the opposite direction. In Fig. 10 are displayed values of the measured impedance for the $Fe_{72}Cu_1V_4Si_{15}B_8$ alloy sample annealed at $500^\circ C$ at $H_{max} = +21.8$ kA/m and $H_{max} = -21.8$ kA/m where $0.002 \Omega < \Delta Z < 0.1 \Omega$.

Fig. 11 shows frequency dependence of MI ratio of $Fe_{73}Cu_1Nb_3Si_{13.5}B_{9.5}$ microwires for sinusoidal current amplitude of 3 mA performed by the four-point method by Hioki LCR/HiTester [12]. Critical frequency of about 30 kHz (when $\delta_m \approx d/2$) was observed as the point with initial increase of MI.

It is important to note that the maximum value of MI ratio is attained at frequency of about 1 MHz, what is crucial to design optimum MI-based sensors [12].

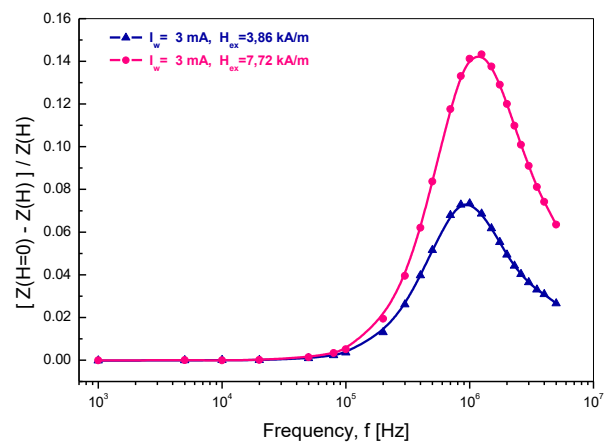


Figure 11. Dependence of the MI ratio on frequency in as-quenched $Fe_{73}Cu_1Nb_3Si_{13.5}B_{9.5}$ microwires for $H'_{ex} = 3.86$ kA/m and $H''_{ex} = 7.72$ kA/m sinusoidal current amplitude 3 mA [11].

Diagrams for the MI ratio dependence on frequency as well as external magnetic field intensity in as-quenched $Fe_{72}Cu_1V_4Si_{15}B_8$ ribbons are shown on Fig. 12 and Fig. 13 respectively, representing the 2-D and 3-D views of the result. Those 3-D diagrams enable complete observation of the MI-ratio interdependence on both parameters.

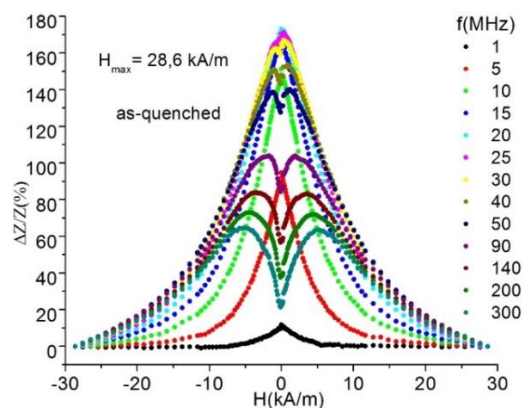


Figure 12. Dependence of the MI ratio on external magnetic field H in as-quenched $Fe_{72}Cu_1V_4Si_{15}B_8$ ribbons [6].

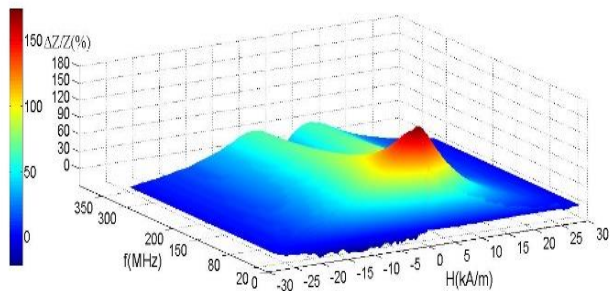


Figure 13. MI ratio in as-quenched $Fe_{72}Cu_1V_4Si_{15}B_8$ ribbons depending on external magnetic field H and frequency f (3-D display) [6].

4. CONCLUSION

Discovery of the MI effect initiated research of the materials in which this effect is the most expressive. It is possible to create a very sensitive magnetic field sensor that can be applied in various industrial, medical and biological spheres where the requirements for the acquisition of changes in the magnetic field are very strict, just by producing iron and cobalt based alloys. Modern scientific trends are focused on material research in order to produce miniature devices with the same or improved characteristics. The study of MI effect gives a positive contribution to education in the field of physical sciences, because this effect brings together several scientific disciplines, which makes it multidisciplinary. Educations that include the study of MI effects are materials science, electrical engineering as well as informatics.

The idea is to educate scientific staff for the design, structural and physical analysis of the materials in which the MI effect exhibits and to give a contribution to the choice of principle of measuring depending on the frequency at which the effect occurs.

REFERENCES

- [1] L.V. Panina, K. Mohri, (1994). "Magneto-impedance effect in amorphous wires", Applied Physics Letters, 65, 1189–1191.
- [2] L. Kraus, (1999). "Theory of giant magneto-impedance in the planar conductor with uniaxial magnetic anisotropy", Journal of Magnetism and Magnetic Materials, 195, 764–778,
- [3] L. Kraus, Z. Frait, K.R. Pirota, H. Chiriac (2003). "Giant magnetoimpedance in glass-covered amorphous microwires", Journal of Magnetism and Magnetic Materials, 254–255, 399–403.
- [4] D. Menard, M. Britel, P. Ciureanu, A. Yelon (1998). "Giant magnetoimpedance in a cylindrical magnetic conductor", Journal of Applied Physics, 84(5), 2805–2814.
- [5] M. H. Phan, H-X. Peng, (2008). "Giant magnetoimpedance materials: fundamentals and applications", Progress in Materials Science, 53, 323–420.
- [6] R. Surla, N. Mitrović, S. Djukić, V. Ibrahimović (2016). "Amorphous $Fe_{72}Cu_1V_4Si_{15}B_8$ ribbons as magneto-Impedance sensing element", Serbian Journal of Electrical Engineering, 13(3), 381-394 DOI:10.2298/SJEE1603381S.
- [7] M. Knobel, M. Vázquez and L. Kraus (2003). "Giant magnetoimpedance", K.H.J. Buschow, "Handbook of magnetic materials", 497- 563.
- [8] H. Chiriac and T.A. Ovari (1996). "Amorphous glass-covered magnetic wires: preparation, properties, applications". Progress of Materials Science, 40, 333–407.
- [9] M. Knobel, M. L. Sanchez, C. Gomez-Polo, P. Marin, M. Vazquez, and A. Hernando, (1996). "Giant magnetoimpedance effect in nanostructured magnetic wires", Journal of Applied Physics 79 (3), 1646–1654.
- [10] M. H. Phan, H. X. Peng, (2008). "Giant magnetoimpedance materials: Fundamentals and applications", Progress in Materials Science 53, 323–420.
- [11] Agilent Technologies, (2009). "Impedance Measurements", February, 2009, 5989-9887EN.
- [12] N. Mitrović, J. Orelj, A. Milovanović (2016). "Magnetoimpedance effect in FINEMET microwires for sensors applications", The 5th Conference »Advanced Ceramics and Application«, New Frontiers in Multifunctional Material Science and Processing, September 21-23, Belgrade, Book of Abstracts pp. 69-70.